IET Signal Processing

Research Article

IET Journals
The Institution of Engineering and Technology

Classification of Doppler radar reflections as preprocessing for breathing rate monitoring

ISSN 1751-9675
Received on 15th January 2018
Revised 21st June 2018
Accepted on 17th July 2018
E-First on 8th October 2018
doi: 10.1049/iet-spr.2018.5245
www.ietdl.org

Isar Nejadgholi[1], Hamidreza Sadreazami[1], Sreeraman Rajan[2] ✉, Miodrag Bolic[1]

[1]*School of Electrical Engineering and Computer Science, University of Ottawa, Ottawa, Canada*
[2]*Department of Systems and Computer Engineering, Carleton University, Ottawa, Canada*
✉ *E-mail: sreeramanr@sce.carleton.ca*

Abstract: Classification is presented as a pre-processing step in this study. The state of the subject is classified as the unmoving state with normal breathing (normal breathing class), unmoving state with no breathing (stop breathing class) or the state when the subject is moving (erratic signal class) before breathing estimation algorithms are applied. Estimation algorithms may be applied to obtain breathing rate if normal breathing class is detected or alarms may be generated if stop breathing is detected, and fine-grained classification of activities may be pursued if the erratic signal is detected. Experiments were performed using a single-channel pulse-modulated continuous wave radar with three subjects for a total of 135 min. In each experiment, the subject was continuously monitored for 15 min and the subject performed activities that resulted in a signal that belonged to one of the three classes. Besides extracting a feature that assessed the distribution of energy of the signal in the frequency domain, a novel nonlinear time series feature extraction method based on the higher-dimensional embedding technique was applied to ascertain periodicity of the reflected signal. Bayes classifier was used to classify each 5-s segment of radar returns. A 30-fold cross validation resulted in 97% of overall classification accuracy.

1 Introduction

In the past, radars were used in military applications mostly for air defence and as a sensor for passenger airplane location and guidance in civilian applications. Nowadays, radars are increasingly used as a sensor for breathing rate monitoring, because they are contactless, privacy friendly and generally safe. Contactless monitoring using passive sensors such as video cameras invades the privacy of people and does not perform well in the absence of a line of sight [1, 2]. On the other hand, radars can penetrate occlusions depending on the frequency of transmission and the type of occlusion [3]. Hence, radars are more versatile contactless sensors for monitoring vital signs. Radars are currently being used as contactless, standoff sensors in various civilian applications such as fall detection of elderly people in residential care facilities [4], detection of attempted suicide events in prisons [5], monitoring of respiration and heart activity in nursing care facilities [6] and finding human subjects in search and rescue applications [7]. Essentially, radars are penetrating the biomedical sector as a useful remote health monitoring sensor.

The proposed work is a part of a larger project whose eventual goal is to perform long-term monitoring of elderly people and inmates. In this context, monitoring includes estimating the breathing rate while the subject is not moving and classifying the types of activities when the subject is moving and generating an alarm in the case when fall or other dangerous event is detected such as an attempt of a suicide in prison. Our previous work, therefore, led to publications where breathing was estimated when the subject was not moving [8] and when the subject was walking [9] and very fine-grained classification of activities was done with more than 40 features [10]. However, for this work and any other work that involves real-time and long-term monitoring, it is important to detect the state or activity of the subject before applying other signal processing algorithms. For example, breathing estimation algorithms mainly assume that the person is not moving and that the signal is stationary. Hence breathing estimation may be attempted only after ensuring that the person is not moving. This study aims to develop a preprocessing step using classification where only course-grained classes will be determined based on a small set of features. Subsequent to this preprocessing step, appropriate signal processing steps may be undertaken.

Both ultra-wideband (UWB) and continuous wave (CW) radar systems have been used for non-contact health monitoring. CW radars utilise the Doppler shifts in the reflected signals off the subjects to estimate the breathing and heart rate. Fourier spectrum analysis is often used to estimate breathing and heart rate from the CW radar signal reflected from the chest and peaks of harmonics are interpreted as estimates of breathing and heart rate [11–14]. Interestingly, almost all the existing works in the literature was carried out assuming that the subject is stationary and breathing normally. When the subject is stationary and alive but has stopped breathing, Fourier analysis may still present a peak frequency in the range of breathing due to the noise harmonics which can be misleading [15, 16]. As a consequence, Fourier analysis may not be able to accurately detect the cessation of breathing. However, it is very important to recognise this state and to generate alarms. Before conducting any Fourier analysis, care needs to be taken to ensure that there is no Doppler contribution due to the motion of other body parts. Alternatively, it is necessary to ascertain if linear or nonlinear signal analysis should be undertaken as a first step towards processing the signal. To the best of our knowledge, such identification or classification is not commonly considered as part of preprocessing.

In general, more advanced signal processing methods are needed to extract the information related to breathing [17–20]. Only recently the role played by the radar cross section (RCS) of the human body in the design of the system and algorithms was investigated in [21]. Although the role of RCS was studied for stationary subjects, this work provided no guidance for the development of signal processing methods. Furthermore, in [22], a noncontact UWB impulse radar-based approach was proposed for sleep apnea detection. Experimentation was done in sitting position at varying distances from the radar to ascertain the estimation accuracy of the amplitude of chest motion. Since short impulse radio signals were used as radar signals, multiple peak detection in the time domain was used to ascertain the disposition of the chest and then was followed by regular Fourier analysis. Although the study succeeded in estimating the breathing rate, it could not estimate the breathing rate when there was movement. We

Table 1 Three classes of radar reflections considered in this work

Type of received signal	Source	Further possible action	Potential processing technique
normal breathing	stationary subject with regular breathing	estimation of breathing and heart rate	spectral analysis
erratic	subject with physical activity or irregular breathing	detection or diagnosis depending on the application	fine-grained classification, breathing estimation while moving
stop breathing	alive stationary subject with no breathing	alarming the relevant person and monitoring the heart beat	spectral analysis

recognise this issue and hence we propose a paradigm different from those that exist in the current literature for signal processing of the radar received signals.

In the proposed paradigm, prior to applying any more detailed processing or fine-grained classification on the radar received signal, the received signal is categorised as one of the several classes. Depending on the class, an appropriate method for spectral analysis, estimation or fine-grained classification is carried out. Thus, classification is viewed as a preprocessing step instead of traditional thinking where it is considered as a post-processing step. In this classification task, three types of classes are considered, each of which requires a totally different type of processing. These three classes are (i) *normal breathing*, which is related to an unmoving subject with regular breathing and breathing estimation can be done using spectrum analysis techniques such as Fourier transformation, (ii) *erratic signal* which is related to an irregular breathing signal or the signal corrupted with movement artefacts of the subject which might require finer-grained classification and potentially advanced signal processing algorithms for breathing estimation while walking if walking class is detected (iii) *stopped breathing* which is the absence of breathing pattern due to the holding of the breath or undergoing sleep apnea.

Classification algorithms have been used to distinguish various activities of the monitored subject. In most of these works, a set of human activities were considered and depending on the target classes, different features were extracted mostly from the time and frequency domains and learning algorithms were applied to classify the signal based on extracted features [10, 23–27]. In some applications, the frequency content of the radar signal was divided into different frequency bands representing breathing, heart activity, and body motion, and features were extracted from each band of frequency [5, 28, 29]. In [24, 25, 30], features were extracted from spectrograms of the radar returns to classify them into various activities. A comprehensive set of features was extracted in [10] and feature selection was used to find the most informative and distinguishing features among classes of human activities. Besides studying time and frequency features, researchers have applied other methods of feature extraction using wavelet packets [31], entropy analysis [32] and empirical mode decomposition [33, 34] to monitor and classify human activities.

In this work, we implement a classification algorithm that extracts few relevant and useful features related to breathing patterns contained in the radar reflections and classifies short time segments of radar reflections into one of the classes given in Table 1. According to the American College of Emergency Physicians [35], an adult breathes 12–20 times per minute which is equivalent to 0.2–0.3 Hz. The normal heart rate for healthy adults ranges from 60 to 100 beats per minute (bpm) or 1–1.667 Hz. Therefore, the distribution of the spectrum of the signal in these ranges of frequency contains salient information related to normal breathing. The magnitude of the received signal is also an informative feature since physical activity increases the amplitude of the reflected radar signal and holding the breath decreases it. This feature needs to be normalised properly across subjects and sessions of experiments [36, 37]. Periodicity in the breathing pattern in the reflected signal contains crucial information in order to distinguish between normal breathing and erratic signal. Although movements of the chest caused by breathing and heart beat repeat over time, these movements cannot be considered as purely periodic. For instance, physical activity or irregularity in breathing patterns may affect the periodicity of the signal *or even make it quasi-periodic*. Furthermore, normal and stop breathing may have different periodicities to stop breathing contains only the radar reflections related to movements of the heart in case a subject is not moving. In reality, the order of periodicity of the reflected signal may vary from very close to periodic (stationary subject with normal breathing) to aperiodic (erratic breathing or random body movements) [38]. To obtain an estimate of the periodicity as a feature, the proposed method uses embedding space to process radar reflections from a human.

Embedding space is a powerful tool to estimate the periodicity of natural signals [39]. Although periodicity of natural signals has been estimated from embedding space and used as features in various applications [40, 41], it has not been used before to assess the classification of the type of signal in the received radar reflections.

The paper is organised as follows. The proposed method, as well as detailed explanations of each step, is presented in Section 2. Results obtained from implementing different blocks of the method are presented in Section 3. Section 4 discusses the results and potential applications of the developed method. Also, note that in this work, the term ‘radar signal’ is used interchangeably to mean the output signal obtained from the radar unit used in this work.

2 Proposed methodology

2.1 Experimental setup and data collection

An SR12003 phase-modulated CW (PMCW) radar is used in this project, which is a prototype manufactured by K&G Spectrum (Gatineau, QC, Canada). The radar unit has a 3 dB beamwidth of 120° × 5°, a sampling frequency of 1.48 kHz and an operating frequency of 24.125 GHz. The phase of the transmitted waveform is modulated using a 1023-bit long pseudo-random noise (PN) binary sequence. The clock frequency of the PN sequence is 200 MHz, which is equivalent to a 5 ns sub-pulse width. This radar system delays the transmitted PN sequence by multiples of its clock period and correlates the delayed PN sequence with the received reflections which results in 0.75 m range bins. The carrier frequency is then demodulated from the correlated signal using a low pass filter with a cut-off frequency of 10 kHz and this processed signal is available as an output of the device. All further processing mentioned in this work uses this output signal. A proprietary software, KGScope, provided by K&G Spectrum Inc., was used to control the system and record data. Using this software the radar was set to dwell on a range bin where the target subject was present.

Fig. 1 shows the block diagram of the proposed method. As shown in this block diagram, two kinds of signals are collected in our experiments, namely, radar reflections and respiratory inductance plethysmography (RIP) signal. The RIP band is used to record changes of volume of the chest while the subject is breathing. Radar reflections contain reflections due to all the movements from the subject during the experiments, including those movements of the chest during the experiment.

The RIP band was placed around the subject's thorax. The RIP band was connected to an amplifier (model 15LT Physiodata Amplifier System with 15A54 Quad Amplifier; Grass Telefactor; Warwick, RI, USA). The RIP band signal was amplified with a gain of 200 and a bandwidth of 0.1–30 Hz. The signal acquired from the RIP band was sampled at 1000 Hz using a 16-bit analogue-to-digital converter board (model USB-6216; National Instruments; Austin, TX, USA).

Three male subjects ageing from 23 to 26 with no history of cardiovascular problems or disorder participated in the data collection and each subject repeated the test session three times

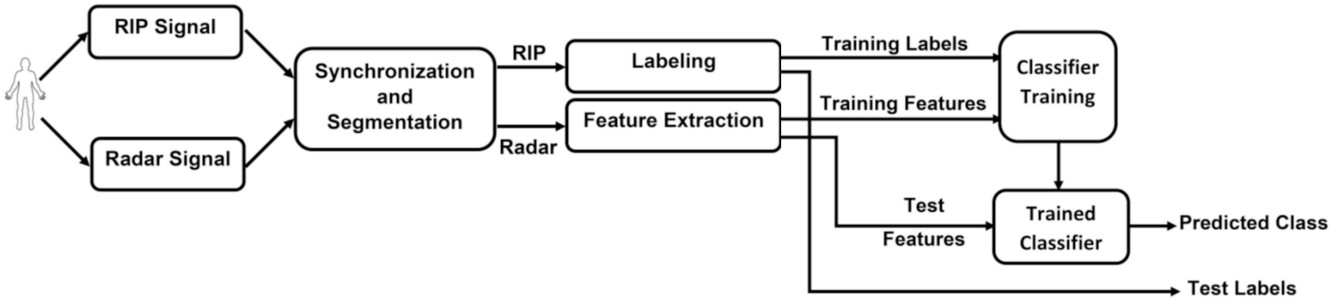

Fig. 1 *Block diagram of the proposed method for classification of radar signals in order to detect the type of received signal. RIP signal is used to assign a label to the corresponding segment of the radar signal. The collected dataset is divided into training and test subsets. Training data is used to train the classifier. Trained classifier is used to predict the class labels for test data and predicted class is compared with test labels to assess the performance of the trained classifier*

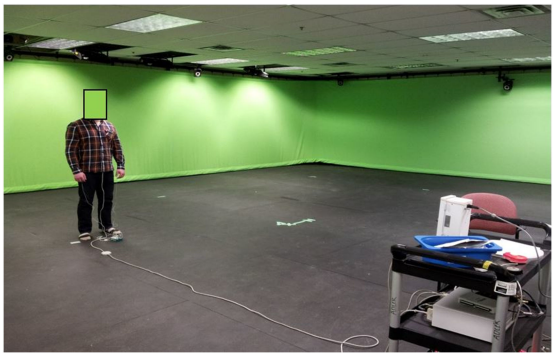

Fig. 2 *View of experiment setup [42]*

[42]. Subjects were standing in front of the radar which was 4 m away. The radar was placed in a horizontal orientation so that the beam spread across the entire subject. Experiments were conducted in a room with wide open space with few sources of reflection. Fig. 2 shows the test setup. The height of the radar was fixed for all experiments. At the beginning and end of each test, the subject was asked to make a *jolting* motion (e.g. quickly standing up and sitting back down). This motion resulted in a sharp abrupt change in the RIP and radar reflected signal and was used to time align the two signals. 135 min of radar return signals and the signal from the RIP band were collected. A single test was 15 min and was broken down into three 5-min sections as follows:

Normal breathing: Subject was in front of the radar as still as possible, breathing normally. The radar reflections recorded in this phase of experiment corresponds to normal breathing.
Physical activity, erratic breathing during recovery, normal breathing: Subject was asked to perform jumping jacks for 30 s to increase the heart rate and breathing rate. For the remaining 4 min and 30 s, the subject was asked to let the breathing and heart rate return to normal. The radar reflections acquired in the first 30 s is erratic due to the physical activity. After the physical activity, the recorded reflections are considered erratic because of irregular breathing as the subject recovers from physical activity. After the recovery phase is passed, the recorded reflections correspond to normal breathing.
Holding breath, erratic breathing during the recovery, normal breathing: Subject was to hold the breath for as long as possible until it is no longer comfortable and then to continue breathing allowing his or her breathing to return to normal. The subject remained as still as possible during the breath hold. The signal recorded in this phase of the experiment is to stop breathing signal. Upon starting to breath, the subject generally starts with deep breathing as a part of recovery from holding the breath. This part of the recovery period is considered as erratic. The reflected signal recorded after the deep breathing phase would contain normal breathing.

The goal of this work is to obtain the class information as described in Table 1. The RIP signal is a reference signal used to label radar reflection segments for training and testing the classifier. RIP and radar reflected signals are first synchronised and segmented in the time domain. Each 5-s segment of RIP is used to label to the corresponding segment of radar reflections, as normal breathing, erratic signal or stop breathing signal. The labelling of the radar reflections is done using an automated process and confirmed/corrected manually (if needed) by carefully matching the timing instructions given to the subjects and labels. Out of 1620 segments, 18 were corrected manually.

Relevant features are extracted from each segment of the radar signal. The collected data is divided into training and test datasets. Features of training data set along with the corresponding labels are used to train the classifier. Features of a test dataset are fed to the trained classifier and the labels of test segments are predicted by the trained classifier. Predicted class labels are then compared with the test labels (assigned using the RIP signal) to measure the confusion matrix including classification accuracy in each class and sensitivity and specificity between classes.

Two methods of cross validation are applied in this work. First, we use K-fold cross validation in which the dataset is divided into K subsets. The model is trained and tested K times. Each time $K-1$ subsets are used as training datasets, while the Kth subset is used to test the classifier. Second, subject cross validation is used in which the data from the two subjects is applied to train the classifier and the data from the third subject is used to test it. While K-fold cross validation assesses how the classification results will generalise to an independent dataset, subject cross validation indicates how it will generalise to the dataset from new subjects who are not included in the training dataset.

2.2 Radar feature extraction

The radar signal is a nonlinear function of chest displacements due to the heart activity and breathing. Distribution of energy in the spectrum was extracted from the frequency domain while periodicity of the signal was extracted from embedding space.

2.2.1 Features extracted in the frequency domain: To obtain the spectrum of each time segment, Welch periodogram is applied [43]. For a time series $x = x_n$, $n = 0, \ldots, N-1$, the power spectrum $P_x(\mathrm{e}^{\mathrm{j}\omega})$ is the Fourier transform of the autocorrelation sequence, written as

$$P_x(\mathrm{e}^{\mathrm{j}\omega}) = \sum_{k=-N+1}^{N-1} r_x(k)\mathrm{e}^{-\mathrm{j}k\omega}, \tag{1}$$

where $r_x(k)$ is the autocorrelation of the signal calculated as

$$r_x(k) = \frac{1}{M}\sum_{n=0}^{N-1} x_{n+k}x_n\,. \tag{2}$$

In this work, the frequency of interest is limited to 0–11.5 Hz. Since the radar reflected signal is a nonlinear function of chest displacements, it contains not only the main harmonics of

breathing and heart rate but also its higher harmonics and inter-modulation components. The fraction of the total energy in a range of frequencies corresponding to breathing to the total energy in the spectrum changes when breathing changes from being normal to erratic or when breathing stops. This ratio is expected to be the largest when breathing is normal. Therefore, a wide range of frequencies instead of a very narrow frequency range corresponding to the breathing frequency is used to extract the relevant power spectrum density (PSD)-ratio feature [44, 45]. The PSD-ratio feature of the radar signal is extracted as the ratio of the energy of the signal in the range of breathing and heart rate (0–2.3 Hz) to the total energy of the signal in a wider range of frequencies (0–11.5 Hz).

2.2.2 Modelling the radar signal in embedding space: Frequency domain processing methods are not able to distinguish between signals that have the same power spectra but different phases and/or higher-order spectra [46]. In a radar system, the received signal is phase modulated due to the movements of the target object. Therefore, it is necessary to search for patterns not only in the time and frequency domains but also in a higher-dimensional transformation of the time series that is able to reveal the phase information. Embedding space is a multi-dimensional space in which a signal is plotted against time-delayed versions of itself. For a time series $x = x_n$, $n = 1, \ldots, N$, each point of the d-dimensional embedding space is defined as

$$\boldsymbol{x}_n = \left[x_{n-(d-1)\tau}, \ldots, x_{n-\tau}, x_n\right], \quad n = (1 + (d-1)\tau), \ldots, N, \tag{3}$$

where τ is the time lag and d is the dimension of embedding space. The entire embedding space is generated by trajectory matrix $\boldsymbol{X}$ defined as

$$\boldsymbol{X} = \begin{bmatrix} \boldsymbol{x}_{1+(d-1)\tau} \\ \boldsymbol{x}_{2+(d-1)\tau} \\ \vdots \\ \boldsymbol{x}_N \end{bmatrix} = \begin{bmatrix} x_{1+(d-1)\tau} & \cdots & x_{1+\tau} & x_1 \\ x_{2+(d-1)\tau} & \cdots & x_{2+\tau} & x_2 \\ \vdots & \ddots & \vdots & \vdots \\ x_N & \cdots & x_{N-(d-2)\tau} & x_{N-(d-1)\tau} \end{bmatrix}. \tag{4}$$

This trajectory matrix is usually referred to as an attractor and is considered as a method for determining the periodicity of nonlinear time series [47, 48]. The strong periodic component of the signal will result in the embedding attractor that occupies less volume in the embedding space.

Dimension and time lag are two parameters used to create the embedding space. In this work, the dimension of the embedding space was set to 2. Since we were able to create distinguishable two-dimensional (2D) embedding spaces for three classes mentioned in Table 1 and we aimed to keep the feature extraction process computationally inexpensive, higher-dimensional embedding spaces were not assessed. The time lag of embedding space is usually calculated by finding the first local minimum of auto-mutual information (AMI) or the first zero-crossing of the autocorrelation function between a time series and its delayed versions [49]. In the proposed method, we use AMI to estimate the time lag, since it provides a more appropriate delay value [48, 50, 51]. This is due to the fact that AMI is capable of measuring nonlinear dependencies, which are the case in radar breathing data. A low value of AMI results when there is little information common between the two time series. To construct the embedding space, a number of time lags are considered as candidates. For a candidate time lag τ, the AMI between time series $x = x_n$ and $y = y_m = x_{n-\tau}$ is calculated as

$$\mathrm{AMI}(x, y) = \sum_{n,m} p(x_n, y_m) \log \frac{p(x_n, y_m)}{p(x_n)p(y_m)}, \tag{5}$$

where $p(x_n)$ is the probability of measuring a data value x_n, $p(x_n, y_m)$ is the joint probability of measuring x_n and y_m. To extract probability density functions mentioned in (5), the range between the minimum and maximum of the time series is first divided into a finite number of non-overlapping sub-intervals. Then, the histogram method, which is based on counting the relative occurrences of the time series values within each sub-interval is used [52]. AMI is maximum for $\tau = 0$, which is equal to the entropy of time series. As time lag increases from zero, AMI decreases. However, depending on the periodicity of the signal, AMI starts to oscillate for time delays bigger than a certain point. The first local minimum of the AMI curve versus candidates of time lag is taken as the proper time lag for constructing the embedding space [53].

After constructing the trajectory matrix, the attractors constructed for various classes are modelled and parameters of the model are extracted as features of the signal in the embedding space. For low-dimensional attractors, the model can be chosen heuristically.

Here, linear regression is used to model the 2D attractors obtained in embedding space and use the parameters that indicate goodness of the fit as features of the radar-reflected signal in embedding space. More details about extracted features from embedding space are given in Section 3.3.

3 Results

3.1 Segmentation

135 min of RIP and radar signals are recorded as explained in Section 2.1. The sampling frequency is 1 kHz for the RIP signal and 1.48 kHz for the radar reflected signal. Two signals are synchronised using the signature of jolting motion at the beginning of recordings. The signals are segmented into 5-s intervals. Fig. 3 shows an example of radar segments for each type of breathing in both time and frequency domains. We chose extreme examples to show the difference between three types of recorded radar reflected signals. RIP signal segments are used to label the type of the corresponding segment in the radar signal.

3.2 Radar feature extraction in time and frequency domains

The signal output from the radar device ('radar signal') is down-sampled by a factor of 10. Each 5-s interval is smoothed using a moving average filter with the window length of 0.07 s and the variance of the signal is calculated. Then each segment is normalised using the equation $x = (x - \mu)/\sigma$ and the Welch periodogram of the signal is calculated with 2-s sub-segments and 1-s overlap. In the frequency domain, the ratio of PSD in the range of 0–2.3 and 0–11.5 Hz is calculated as an index of the energy of breathing harmonics to the energy of other harmonics existing in the signal. Fig. 3 shows three segments of the signal in time and frequency domains labelled as stop breathing, normal breathing, and erratic signal. The PSD-ratio feature is 0.50 for stop breathing, 0.22 for erratic breathing, and 0.86 for normal breathing, respectively. The PSD-ratio is a distinguishing feature for these three classes of signals. The PSD-ratio has a low value for erratic breathing since the erratic signal has high-magnitude harmonics outside the range of breathing frequencies. On the other hand, the PSD-ratio is high for normal breathing because the highest harmonics of normal breathing signals are located in the range of breathing frequencies. For stop breathing, there is a peak in the frequency range of heart beat. In this case, the energy of the spectrum is distributed over the range of 0–5 Hz, therefore the PSD-ratio feature is not as high as normal breathing and not as low as the erratic signal.

3.3 Feature extraction in embedding space

Down-sampled and normalised received radar reflected signal segments are transformed to 2D embedding space with a time lag of 0.1 s. Fig. 4 shows the AMI graph versus a range of candidate number of samples (time lags). From this graph, we see that the first local minimum occurs in about $\tau = 0.1$ or delay of 15 samples. As stated in Section 2.2.2, the periodicity of the signal can be indicated by the characteristics of the constructed attractor in embedding space. We know that the normal breathing pattern is close to periodic, while the erratic signal does not exhibit a

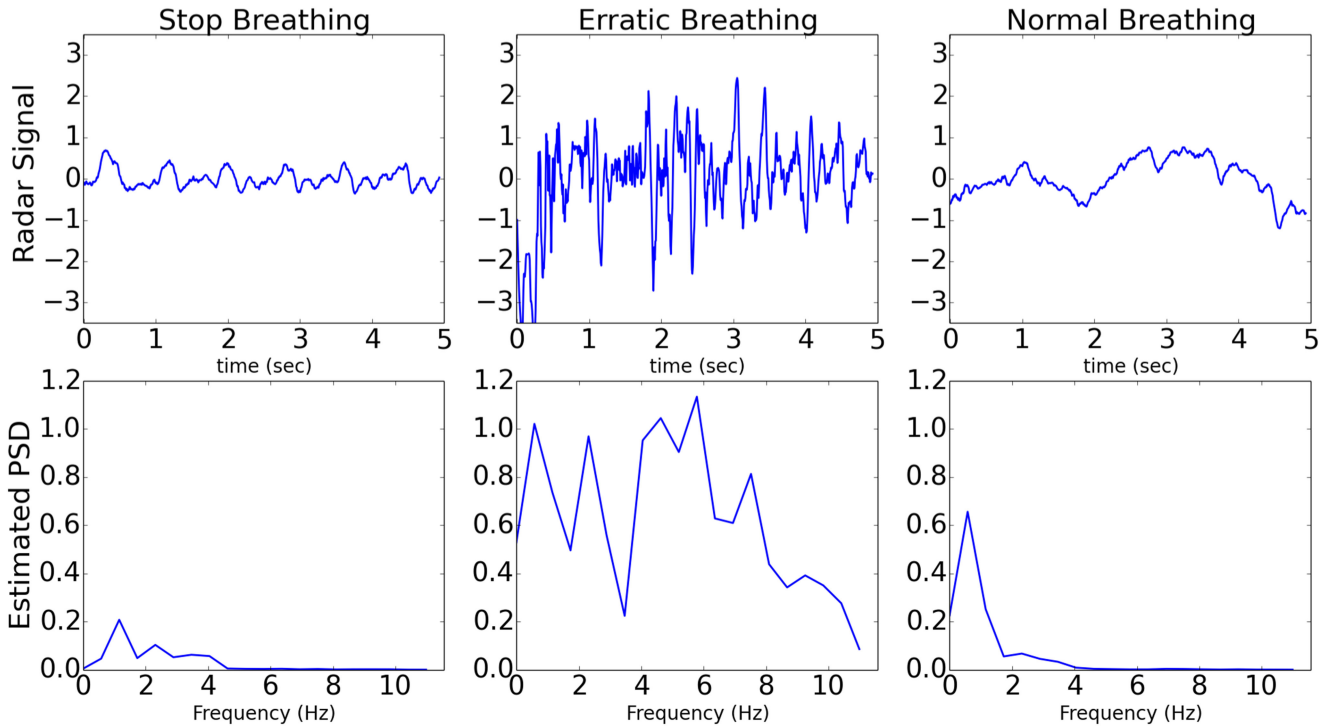

Fig. 3 *Examples of three types of radar signals in time and frequency domains*

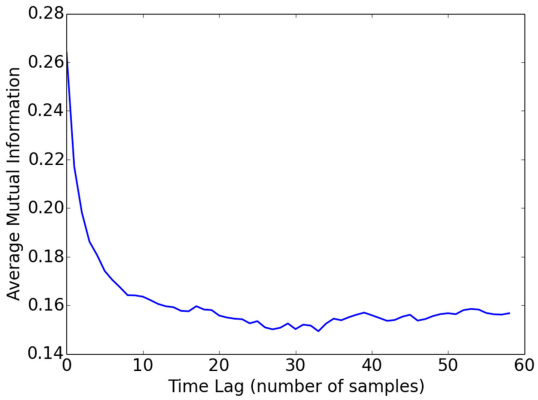

Fig. 4 *Average of mutual information versus time lag. The first local minimum of mutual information happens when time lag is 15 samples or 0.1 s*

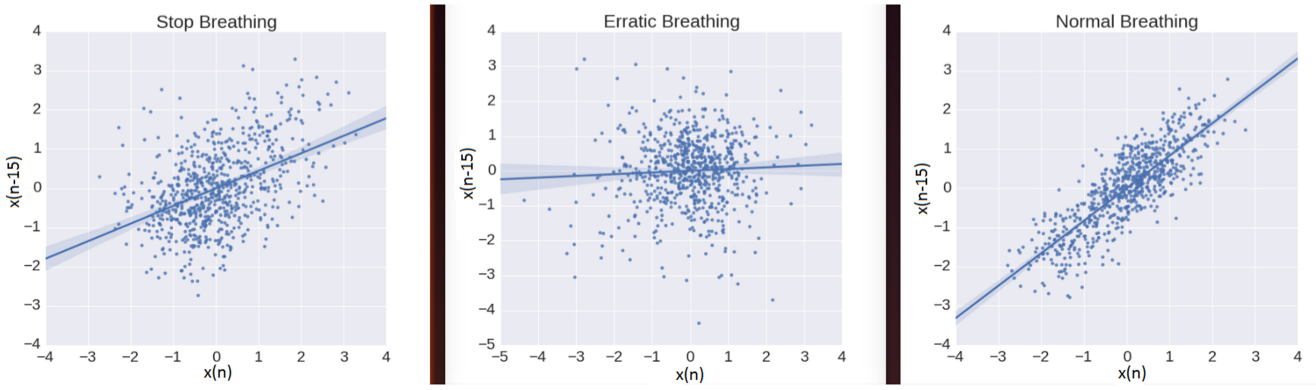

Fig. 5 *Embedding space for samples shown in Fig. 3 when normalised in the time domain. The embedding spaces are modelled with linear regression and three features that describe the goodness of fit are extracted*

periodic pattern. We used linear regression to extract features of these attractors. The fitted linear models are also shown in Fig. 5. Comparing three segments of the signal as shown in Fig. 3 (time and frequency domains) and Fig. 5 (embedding space), illustrates how periodicity of signal manifests in embedding space for this specific type of signal.

Different features can be extracted from the linear model of embedding space. The slope of the fitted line shows the correlation between the time series with a delayed version of it. The goodness of linear fit is used as an indication of periodicity. For the three example segments of the signal shown in Fig. 3, the obtained correlation is 0.45, 0.05 and 0.82 for stop breathing, erratic signal, and normal breathing, respectively. To measure the goodness of fit, we extract two parameters, which are normalised variance of linear regression and the sum of residuals. The closer variance of fit to 1 is, the better fit we have achieved. This parameter is 0.2, 0.00 and

Table 2 Summary of features (mean ± Std)

Class	Count	PSD-ratio (section 3.2)	Variance of regression	$R(\boldsymbol{X})$ in (6)
stop	67	0.61 ± 0.18	0.20 ± 0.17	1.13 ± 0.65
erratic	114	0.36 ± 0.24	0.13 ± 0.24	0.02 ± 0.04
normal	1439	0.93 ± 0.06	0.80 ± 0.13	0.06 ± 0.13

Table 3 Confusion matrix for 30-fold cross validation

Label	Prediction			
	Normal	Erratic	Stop	Sum
stop	2 (3%)	0 (0%)	65 (97%)	67
erratic	4 (3.5%)	109 (95.6%)	1 (0.9%)	114
normal	1404 (97.6%)	4 (0.3%)	31 (2.1%)	1439

Table 4 Confusion matrix for subject excluded training

Label	Prediction			Sum
	Normal	Erratic	Stop	
stop	2 (3%)	0 (0%)	65 (97%)	67
erratic	5 (4.3%)	101(88%)	8 (7.0%)	114
normal	1404 (97.6%)	4 (0.3%)	31 (2.1%)	1439

Table 5 Confusion matrix when normal breathing segments include RBMs

Label	Prediction			Sum
	Normal	Erratic	Stop	
stop	2 (3%)	0 (0%)	65 (97%)	67
erratic	4 (3.5%)	109 (95.6%)	1 (0.9%)	114
normal	871 (61%)	565 (39%)	3 (0%)	1439

0.68 for stop breathing segment, erratic segment, and normal breathing segment shown in Fig. 3, respectively. From Fig. 5, we observe that the sum of residuals is low for normal breathing, higher but relatively similar to stop breathing and erratic signal. The reason why stop breathing and erratic breathing look the same in terms of residuals is that we normalised the segments in the way explained in Section 3.2. Normalisation is necessary for comparing the correlation and variance of linear regression. However, the residuals of linear regression for stop breathing are much smaller than the residuals in case of erratic breathing in terms of actual values (without normalising time domain signals). Therefore, in order to make this feature distinguishable between stop breathing and erratic signal, we divided the sum of residuals by the variance of the time domain signal. The resulted feature can be written as

$$R(\boldsymbol{X}) = \frac{\sum_{n=1}^{N-1} \mathrm{res}^2(x_n)}{\sigma^2}, \tag{6}$$

where $\boldsymbol{X}$ is the 2D embedding space constructed for the time series $x = x_n$, $n = 1, \ldots, N$, which was described in (3). This 2D embedding space is fitted to a line using linear regression as shown in Fig. 5 and $\mathrm{res}(\boldsymbol{x}_n)$ is the residual of linear regression corresponding to point $\boldsymbol{x}_n$ of the embedding space. The scalar σ^2 is the variance of x in the time domain before normalisation. For the three segments of the signal shown in Fig. 3, this parameter is calculated as 0.8, 0.01 and 0.11 for stop breathing, erratic signal, and normal breathing, respectively.

3.4 Classification results

Three features, namely, PSD-ratio, variance of linear regression in embedding space and $R(\boldsymbol{X})$ were selected. Table 2 summarises the extracted features for three classes of breathing patterns.

Bayes classifier is chosen as the classifier as the dataset is unbalanced. Bayes classifier is often preferred for classification in case of unbalanced dataset [54]. This classifier fits a Gaussian distribution to the features and as far as the number of class instances (or samples of a particular class) is sufficient to approximate the Gaussian distribution. Classification accuracy which is defined as the ratio of the number of correctly predicted labels to the number of samples in the dataset is not dependent on the actual size of each class and is dependent on the overlap between the distributions that describe the classes. Although independency of features and normal distribution are assumed while designing a Bayes classifier, it has been shown that this classifier performs well in terms of classification accuracy even when these assumptions are violated [55]. The three above mentioned features were fed to the Bayesian classifier and a 30-fold cross-validation was used to validate the classifier. The overall classification accuracy of 97% for stop breathing event was obtained. The confusion matrix is given in Table 3.

To investigate whether the classifier is over-trained by the features of training subjects, subject-excluded training is carried out and the trained classifier is tested by the features of the excluded subject. In this method, for each subject involved in this dataset, a classifier is trained using the features extracted from other subjects. The result of testing these classifiers is shown in Table 4. The overall classification accuracy, in this case, is still 97%. However, this table shows when the received radar reflected signal is erratic, subject independent classifier results in more false alarms because it misclassified the classes, erratic signal and stop breathing.

The effect of random body movement (RBM) on the performance of the proposed breathing signal classification method is also investigated. To this end, we consider the radar signal model discussed in [9] to model RBMs such as swaying. In particular, for a subject in standing position, the radar baseband signal, $s(t)$, can be modelled as

$$s(t) = a\cos\left(\frac{2\pi}{\lambda}(2d_B(t) + 2d_H(t) + 2d_{\mathrm{RBM}}(t))\right), \tag{7}$$

where a is the amplitude, λ is the wavelength of the PMCW radar, $d_B(t) = B\sin(2\pi f_B t)$, $d_H(t) = H\sin(2\pi f_H t)$ and $d_{\mathrm{RBM}}(t) = R\sin(2\pi f_{\mathrm{RBM}} t)$ represent displacements of chest due to the breathing and heart beats, and RBMs, respectively, B and H are the maximum displacement of the chest due to these movements, R is the amplitude of the RBM signal and f_B, f_H and f_{RBM} are breathing, heart beat and RBM signal frequencies, respectively. For the sake of simplicity, no additive noise is considered in the model. Inspired by this model, a pseudo-random sinusoidal signal is integrated into our radar return signals. To this end, $d_{\mathrm{RBM}}(t)$ is integrated into each radar data segments corresponding to the normal breathing to investigate the effect of RBMs on the normal breathing classification. Inspired by this model, a pseudo-random sinusoidal signal is integrated into our radar signals. To this end, $d_{\mathrm{RBM}}(t)$ is integrated into the segments of each radar data that correspond to the normal breathing to investigate the effect of RBMs on the normal breathing classification. Table 5 gives the confusion matrix when the radar signal x, obtained during normal breathing, includes RBMs, where $R =$ max (x) and $f_{\mathrm{RBM}} = 1$ Hz. This is a challenging case because the amplitude of swaying is at least as high as the amplitude of breathing [56]. It is noted that spectral analysis of postural sway has revealed that its vast majority of energy is below 1 Hz [57]. It is seen from this table that, as expected, by integrating RBMs in the received radar data the number of confusions between normal and erratic breathing increases.

Next, $d_{\mathrm{RBM}}(t)$ is integrated into the segments of the radar data corresponding to the stop breathing to investigate the effect of RBMs on the stop breathing classification. Table 6 gives the confusion matrix when the radar signal x, obtained during stop breathing, includes RBMs, where $R =$ max (x) and $f_{\mathrm{RBM}} = 1$ Hz. It is seen from this table that RBMs result in confusion between the stop and erratic breathing signals.

Regarding computational complexity, it is noted that the proposed method is computationally efficient since the training is done off-line. Required central processing unit time during testing

Table 6 Confusion matrix when stop breathing segments include RBMs

Label	Prediction			Sum
	Normal	Erratic	Stop	
Stop	2 (3%)	8 (12%)	57 (85%)	67
erratic	4 (3.5%)	109 (95.6%)	1 (0.9%)	114
normal	1404 (97.6%)	4 (0.3%)	31 (2.1%)	1439

is 0.084 s on an Intel Core i7 2.93 GHz personal computer with 16 GB RAM.

4 Discussion

Current radar-based vital sign monitoring systems can only estimate breathing when the subject is stationary and breathing normally. Monitoring breathing rate of human subjects during physical activity or with irregular breathing is still in its early stages of research. This study presents a different paradigm for monitoring breathing while the subjects are moving or when there is irregular breathing. Instead of estimating breathing, this study proposes to identify if the received radar reflected signal belongs to one of the three classes, namely normal, erratic or stop breathing. Once the signal has been identified as belonging to one of the three classes, appropriate signal processing techniques may be applied to estimate the breathing frequency. For instance, if the signal is classified as normal breathing, then Fourier transform may be applied to estimate the breathing rate. If the signal is classified as stopped breathing, then an alarm may be generated as a precaution. Spectral analysis using Fourier transform will then provide an estimate of heart rate. However, when the signal is classified as erratic breathing, then Fourier transform should not be applied and the time-frequency approach such as the one described in [9] may be considered. Unlike the traditional methods where classification is attempted as a final stage of the signal processing chain, in this work, it is treated as part of the pre-processing stage which would enable an appropriate choice of a class-dependent signal processing algorithm.

It has been shown in [42, 58, 59] that the breathing rate estimation error is the highest when the subject is standing, while it is the lowest when the subject is lying down on the bed. In other words, the breathing rate estimation when the subject is lying down is generally more accurate than when the subject is in the standing position as there is almost no contribution by other small movements such as swaying. In view of this, the proposed method has focused on the more challenging case of standing position in order to categorise the radar breathing signals. As shown through our simulations when swaying has spectral components closer to those of breathing, classification becomes challenging. This also further establishes the premise of the study that signal processing such as spectral analysis should not be applied blindly to the radar signals and a class-dependent signal processing approach should be adopted.

Supervised training of the classifier is achieved using the labels given to each 5-s segment of the signal recorded from the RIP band simultaneously with the radar signal. To extract relevant information from radar reflections, which are able to distinguish the three classes of the received signals (explained in Table 1, we considered the distribution of energy of the signal in the frequency domain. For normal breathing signal, energy was concentrated in the range of breathing frequencies however, for the other classes, a wider distribution of energy was observed.

Embedding space analysis was used in this work to distinguish between classes. The embedding space constructed from the received radar reflected signal related to a periodic normal breathing can be accurately modelled by a linear regression, while the other two types of signals result in low measures of goodness of fit. Therefore, the goodness of fit of the linear model of embedding space is chosen as the other distinguishing characteristics among classes.

Bayes classifier is chosen to perform classification. Bayes classifier is computationally inexpensive and outperforms many other kinds of classifiers in case of the unbalanced dataset since it forms a distribution out of samples of each class. Once the distribution is formed, the classification accuracy is not dependent on the size of each class. In this work, we use 30-fold cross validation to make sure that there are enough points of minor classes (96% of samples) to form the distribution properly. The proposed classifier is tested in both subject-dependent and subject-independent cases and overall accuracy of 97% is achieved in both cases. However, slightly more false alarms are generated while the classifier is subject-independent. The performance gap between these two classifiers will be narrower if a larger dataset with more subjects can be used to train the classifiers. In this work, we chose to perform a hard decision for each class sample and assigned a unique class label to it, since we mainly aimed to introduce the concept and show the importance of classification of signals before any further processing is undertaken. It should be noted that the decision output of the Bayes classifier is the probability of belonging to each class for each data sample. In real applications, instead of relying on a hard decision, a combination of probabilities of belonging to three classes may be used to adjust further analysis of the signal.

The main contribution of this work is to propose a different paradigm where classification is considered as a preprocessing step that can be used before any estimation process is undertaken such as in a radar-based vital sign monitoring system. In this study, it is demonstrated that even in the most favourable case, where a subject is facing the radar, the estimation of the breathing rate using Fourier transform becomes unreliable, if breathing becomes erratic. Hence, classification needs to be carried out before any estimation can be attempted. Unlike, previous classifiers reported on the classification of human activities, this classifier monitors the subject continuously and provides a decision for transient segments of the signal. The proposed approach has the potential for generating alarms when cessation of breathing is detected by the classifier. Note that this classifier makes a decision for each 5-s of reflected radar signals which is a very short time interval. To have a robust alarm generation, detection of consecutive stop breathing segments may be in order. This strategy will significantly decrease the probability of false alarms.

In this study, a single subject was monitored. One of the applications of interest is to monitor a subject (an inmate or elderly) when he or she is alone. Our approach can be extended to monitoring more than one subject, which is left as work for the future. Experiments were performed with a PMCW single channel radar. This radar does not support coherent processing and hence, introduced nonlinearities. However, our classification was reasonably accurate regardless of these inherent nonlinearities. The transmitted radar signal had a narrow beamwidth so that it was capable of focusing on the subject's chest at the distance of several metres. The subject was always in the same range bin (distance from the radar) and the movements did not include walking. It is noted that walking belongs to the same class as the erratic signal and would represent the signal of higher energy and lower periodicity than breathing signal. In this study, we focused on the problem where the person was at one place doing some activities while being at approximately the same distance from the radar. Readers should note that this work has exposed the vulnerability to incorrect estimations when ‘one size fits all’ approach to the signal processing of radar signals is adopted.

In this work, different postures of subjects and relative orientations between the subjects and the radar were not recorded. In the experiments conducted in this work, subjects were facing the radar directly and positioned at a fixed distance. Change of orientation or position will affect the features and hence, the classification results. This has been deferred for future research.

The length of segment for analysis has intuitively been chosen to be 5-s in this work. The length of the signal needs to be long enough, so that the segment of the signal carries enough information about the low-frequency movements of the chest. On the other hand, we need to make decisions quickly so that remedial actions can be taken immediately for life threatening conditions. False alarms can be reduced by intelligently merging consecutive decisions of the algorithm. Such an attempt using the adaptive

length of segments or overlapping windows will be investigated as part of our future work.

5 Acknowledgments

The authors would like to thank Mr Philip Tworzidlo and Dr Adrian Chan for experimental design and data collection and for providing us with the data. We would also like to thank Correctional Services Canada for funding this project.

6 References

[1] Paton, J., Jenkins, R.: 'Suicide and suicide attempts in prisons', in '*Prevention and treatment of suicidal behaviour: from science to practice*' (Oxford University Press, Oxford, 2005), pp. 307–334

[2] Patil, P.B., Chapalkar, S., Dhamne, N.D., *et al.*: 'Monitoring system for prisoner with GPS using wireless sensor network', *Int. J. Comput. Appl.*, 2014, **91**, (13), pp. 28–31

[3] Chen, K., Huang, Y., Zhang, J., *et al.*: 'Microwave life-detection systems for searching human subjects under earthquake rubble or behind barrier', *IEEE Trans. Biomed. Eng.*, 2000, **47**, (1), pp. 105–114

[4] Liu, L., Popescu, M., Skubic, M., *et al.*: 'Automatic fall detection based on Doppler radar motion signature'. Proc. Int. Conf. on Pervasive Computing Technologies for Healthcare, Dublin, 2011, pp. 222–225

[5] Graichen, C., Ashe, J., Ganesh, M., *et al.*: 'Unobtrusive vital signs monitoring with range-controlled radar'. IEEE Signal Processing Medicine and Biology Symp., New York, NY, 2012, pp. 1–6

[6] Suzuki, S., Matsui, T., Kagawa, M., *et al.*: 'An approach to a non-contact vital sign monitoring using dual-frequency microwave radars for elderly care', *J. Biomed. Sci. Eng.*, 2013, **6**, (7), p. 704

[7] Burchett, H.: 'Advances in through wall radar for search, rescue and security applications'. Proc. IET Conf. on Crime and Security, London, 2006, pp. 511–525

[8] Mabrouk, M., Rajan, S., Bolic, M., *et al.*: 'Human breathing rate estimation from radar returns using harmonically related filters', *J. Sens.*, 2016, **2016**, pp. 1–7

[9] Nejadgholi, I., Rajan, S., Bolic, M.: 'Time-frequency based contactless estimation of vital signs of human while walking using PMCW radar'. Proc. IEEE 18th Int. Conf. on e-Health Networking, Applications and Services, Munich, 2016

[10] Forouzanfar, M., Mabrouk, M., Rajan, S., *et al.*: 'Event recognition for contactless activity monitoring using phase-modulated continuous wave radar', *IEEE Trans. Biomed. Eng.*, 2017, **64**, (2), pp. 479–491

[11] Girao, P., Postolache, O., Postolache, G., *et al.*: 'Microwave Doppler radar in unobtrusive health monitoring', *J. Phys.: Conf. Ser.*, 2015, **588**, (1), pp. 012–046

[12] Droitcour, A.D., Boric-Lubecke, O., Kovacs, G.T.A.: 'Signal-to-noise ratio in Doppler radar system for heart and respiratory rate measurements', *IEEE Trans. Microw. Theory Tech.*, 2009, **57**, (10), pp. 2498–2507

[13] Chioukh, L., Boutayeb, H., Deslandes, D., *et al.*: 'Noise and sensitivity of harmonic radar architecture for remote sensing and detection of vital signs', *IEEE Trans. Microw. Theory Tech.*, 2014, **62**, (9), pp. 1847–1855

[14] Girbau, D., Lázaro, A., Ramos, A., *et al.*: 'Remote sensing of vital signs using a Doppler radar and diversity to overcome null detection', *IEEE Sens. J.*, 2012, **12**, (3), pp. 512–518

[15] Kuutti, J., Paukkunen, M., Aalto, M., *et al.*: 'Evaluation of a Doppler radar sensor system for vital signs detection and activity monitoring in a radio-frequency shielded room', *Measurement*, 2015, **68**, pp. 135–142

[16] Chioukh, L., Boutayeb, H., Li, L., *et al.*: 'Integrated radar systems for precision monitoring of heartbeat and respiratory status'. Proc. Asia Pacific Microwave Conf., Singapore, 2009, pp. 405–408

[17] Massagram, W., Lubecke, V.M., Host-Madsen, A., *et al.*: 'Assessment of heart rate variability and respiratory sinus arrhythmia via Doppler radar', *IEEE Trans. Microw. Theory Tech.*, 2009, **57**, (10), pp. 2542–2549

[18] Gu, C., Wang, G., Li, Y., *et al.*: 'A hybrid radar-camera sensing system with phase compensation for random body movement cancellation in Doppler vital sign detection', *IEEE Trans. Microw. Theory Tech.*, 2013, **61**, (12), pp. 4678–4688

[19] Li, C., Lin, J.: 'Random body movement cancellation in Doppler radar vital sign detection', *IEEE Trans. Microw. Theory Tech.*, 2008, **56**, (12), pp. 3143–3152

[20] Mostafanezhad, I., Yavari, E., Boric-Lubecke, O., *et al.*: 'Cancellation of unwanted Doppler radar sensor motion using empirical mode decomposition', *IEEE Sensors J.*, 2013, **13**, (5), pp. 1897–1904

[21] Piuzzi, E., D'Atanasio, P., Pisa Stefano, P., *et al.*: 'Complex radar cross section measurements of the human body for breath-activity monitoring applications', *IEEE Trans. Instrum. Meas.*, 2015, **64**, (8), pp. 2247–2258

[22] Lai, J.C.Y., Xu, Y., Gunawan, E., *et al.*: 'Wireless sensing of human respiratory parameters by low-power ultrawideband impulse radio radar', *IEEE Trans. Instrum. Meas.*, 2011, **60**, (3), pp. 928–938

[23] Kim, Y., Ling, H.: 'Human activity classification based on micro-Doppler signatures using a support vector machine', *IEEE Trans. Geosci. Remote Sens.*, 2009, **47**, (5), pp. 1328–1337

[24] Li, J., Phung Son, L., Tivive, F.H.C., *et al.*: 'Automatic classification of human motions using Doppler radar'. Proc. Int. Joint Conf. on Neural Networks, Brisbane, 2012, pp. 1–6

[25] Tivive, F.H.C., Bouzerdoum, A., Amin, M.G.: 'A human gait classification method based on radar Doppler spectrograms', *EURASIP J. Adv. Signal Process.*, 2010, **2010**, (1), pp. 1–12

[26] Orović, I., Stankovic, S., Amin, M.G.: 'A new approach for classification of human gait based on time-frequency feature representations', *Signal Process.*, 2011, **91**, (6), pp. 1448–1456

[27] Chen, V.C.: 'Doppler signatures of radar backscattering from objects with micro-motions', *IET Signal Process.*, 2008, **2**, (3), pp. 291–300

[28] Cuddihy, P., Ashe, J., Bufi, C., *et al.*: 'Radar based systems and methods for detecting a fallen person', US Patent 8,742,935, June 3, 2014

[29] Ganesh, M., Ashe, J.M., Yu, L., *et al.*: 'Physiology monitoring and alerting system and process', US Patent 8,13/069,483, March 23, 2011

[30] Thayaparan, T., Stankovic, L., Djurovic, I.: 'Micro-Doppler-based target detection and feature extraction in indoor and outdoor environments', *J. Franklin Inst.*, 2008, **345**, (6), pp. 700–722

[31] Avci, E., Turkoglu, I., Poyraz, M.: 'Intelligent target recognition based on wavelet packet neural network', *Expert Syst. Appl.*, 2005, **29**, (1), pp. 175–182

[32] Wang, S., Zhang, D., Bi, D., *et al.*: 'Radar emitter signal recognition based on sample entropy and fuzzy entropy'. Proc. Intelligent Science and Intelligent Data Engineering, Xi'an, 2011, pp. 637–643

[33] Fairchild, D., Narayanan, R.M.: 'Classification of human motions using empirical mode decomposition of human micro-Doppler signatures', *IET Radar Sonar Navig.*, 2014, **8**, (5), pp. 425–434

[34] Narayanan, R.M., Smith, S., Gallagher, K.A.: 'A multifrequency radar system for detecting humans and characterizing human activities for short-range through-wall and long-range foliage penetration applications', *Int. J. Microw. Sci. Tech.*, 2014, **2014**, pp. 1–21

[35] Russell, S., Norvig, P.: 'ER 101: vital signs. American college of emergency physicians'. Available at http://www.emergencycareforyou.org/Emergency-101/Vital-Signs, accessed April 2018

[36] Lindeberg, T.: 'Feature detection with automatic scale selection', *Int. J. Comput. Vision*, 1998, **30**, (2), pp. 79–116

[37] Guyon, I., Elisseeff, A.: 'An introduction to variable and feature selection', *J. Mach. Learn. Res.*, 2003, **3**, pp. 1157–1182

[38] Goldberger, A.L., Rigney, D.R., West, B.J.: 'Chaos and fractals in human physiology', *Sci. Am.*, 1990, **262**, (2), pp. 42–49

[39] Abarbanel, H.: '*Analysis of observed chaotic data*' (Springer Science & Business Media, New York, 2012)

[40] Lahiri, T., Kumar, U., Mishra, H., *et al.*: ;Analysis of ECG signal by chaos principle to help automatic diagnosis of myocardial infarction', *J. Sci. Ind. Res.*, 2009, **68**, (10), p. 866

[41] Kobayashi, T., Madokoro, S., Wada, Y., *et al.*: 'Human sleep EEG analysis using the correlation dimension', *Clin. EEG Neurosci.*, 2001, **32**, (3), pp. 112–118

[42] Tworzydlo, P.: 'Monitoring breathing using a Doppler radar', Master of Applied Science, Carleton University, 2016

[43] Welch, P.D.: 'The use of fast Fourier transform for the estimation of power spectra: a method based on time averaging over short, modified periodograms', *IEEE Trans. Audio Electroacoust.*, 1967, **15**, (2), pp. 70–73

[44] Chioukh, L., Boutayeb, H., Wu, K., *et al.*: 'Monitoring vital signs using remote harmonic radar concept'. Proc. European Radar Conf., Manchester, 2011, pp. 381–384

[45] Li, C., Cummings, J., Lam, J., *et al.*: 'Radar remote monitoring of vital signs', *IEEE Microw.*, 2009, **10**, (1), pp. 47–56

[46] Povinelli, R.J., Johnson, M.T., Lindgren, A.C., *et al.*: 'Statistical models of reconstructed phase spaces for signal classification', *IEEE Trans. Signal Process.*, 2016, **54**, (6), pp. 2178–2186

[47] Little, M.A., McSharry, P.E., Roberts, S.J., *et al.*: 'Exploiting nonlinear recurrence and fractal scaling properties for voice disorder detection', *BioMed. Eng. OnLine*, 2007, **6**, (1), pp. 1–23

[48] Little, M., McSharry, P., Moroz, I., *et al.*: 'Nonlinear, biophysically-informed speech pathology detection'. Proc. IEEE Int. Conf. Acoustics, Speech and Signal Processing, Toulouse, 2006, vol. 2, pp. II–II

[49] Kantz, H., Schreiber, T.: '*Nonlinear time series analysis*' (Cambridge University Press, London, 2004)

[50] Fraser, A.M., Swinney, H.L.: 'Independent coordinates for strange attractors from mutual information', *Phys. Rev. A*, 1986, **33**, p. 1134

[51] Peppoloni, L., Lawrence, E.L., Ruffaldi, E., *et al.*: 'Characterization of the disruption of neural control strategies for dynamic fingertip forces from attractor reconstruction', *PLoS ONE*, 2017, **12**, (2), p. e0172025

[52] Kowalski, A.M., Martin, M., Plastino, A., *et al.*: 'On extracting probability distribution information from time series', *Entropy*, 2012, **14**, (10), pp. 1829–1841

[53] Martinerie, J.M., Albano, A.M., Mees, A., *et al.*: 'Mutual information, strange attractors, and the optimal estimation of dimension', *Phys. Rev. A*, 1992, **45**, (10), p. 7058

[54] Seiffert, C., Khoshgoftaar, M., Van Hulse, J., *et al.*: 'An empirical study of the classification performance of learners on imbalanced and noisy software quality data', *Inf. Sci.*, 2014, **259**, pp. 571–595

[55] Domingos, P., Pazzani, M.: 'On the optimality of the simple Bayesian classifier under zero-one loss', *Mach. Learn.*, 1997, **29**, (2–3), pp. 103–130

[56] Boric-Lubecke, O., Lubecke, V.M., Droitcour, A.D., *et al.*: '*Doppler radar physiological sensing*' (John Wiley & Sons, New Jersey, 2015)

[57] Zhang, T., Valerio, G., Sarrazin, J., *et al.*: 'Impact of random body movements on 60-GHz Doppler radar for real-time monitoring of vital signs'. Proc. 11th EAI Int. Conf. on Body Area Networks, Brussels, 2016, pp. 56–57

[58] Zhang, X.: 'Characterizing performance of the radar system for breathing and heart rate estimation in real-life conditions', Master of Science thesis, Electrical and Computer Engineering, University of Ottawa, 2017

[59] Gunasekara, A.K.I.: 'Contactless estimation of breathing rate using UWB radar', Master of Science thesis, Electrical and Computer Engineering, University of Ottawa, 2017